Supplementary Information: Implementation of an eco-evolutionary approach to photosynthesis and acclimation in the JULES land surface model

Wenyao Gan[1], Martin Best[2], Pier Luigi Vidale[3], I. Colin Prentice[4] and Sandy P. Harrison[1]

1: Department of Geography and Environmental Science, University of Reading, Reading, RG6 6AB, UK
2: Meteorological Office, Fitzroy Road, Exeter, EX1 3PB, UK
3: Department of Meteorology, University of Reading, Reading, RG6 6AB, UK
4: Department of Life Sciences, Georgina Mace Centre for the Living Planet, Imperial College London, Silwood Park Campus, Buckhurst Road, Ascot, SL5 7PY, UK

This Supplementary contains the following information:

Figure S1. Comparison of RMSE of yearly modelled and observed gross primary production (GPP) at yearly scale in (a) humid, (b) semi-arid and (c) arid sites, where humid is defined as an aridity index (AI) <2, semi-arid as AI between 2 and 5, and arid as AI>5.

Figure S2. Simulated and observed seasonal cycle of gross primary production (GPP) at all tropical sites in PLUMBER2.

Figure S3. Simulated and observed seasonal cycle of leaf area index (LAI) at selected FLUXNET sites.

Table S1. Characteristics of the PLUMBER2 sites used in the analyses.

Table S2. Comparison of the performance of PJULES and the JULES-UKESM1 multi-layer model across different PFTs.

Table S3. Summary of seasonal model performance and statistical metrics for Gross Primary Productivity (GPP) in the Northern Hemisphere.

Table S4. Summary of seasonal model performance and statistical metrics for gross primary production (GPP) simulations in the Southern Hemisphere.

Table S5. Summary of seasonal model performance and statistical metrics for latent heat (LE) in the Northern Hemisphere.

Table S6. Summary of seasonal model performance and statistical metrics for latent heat (LE) in the Southern Hemisphere.

Note S1. Photosynthesis in JULES

Note S2. Full description of the sub-daily P model

Figure S1. Comparison of RMSE of yearly modelled and observed gross primary production (GPP) at yearly scale in (a) humid, (b) semi-arid and (c) arid sites, where humid is defined as an aridity index(AI) <2, semi-arid as AI between 2 and 5, and arid as AI>5.

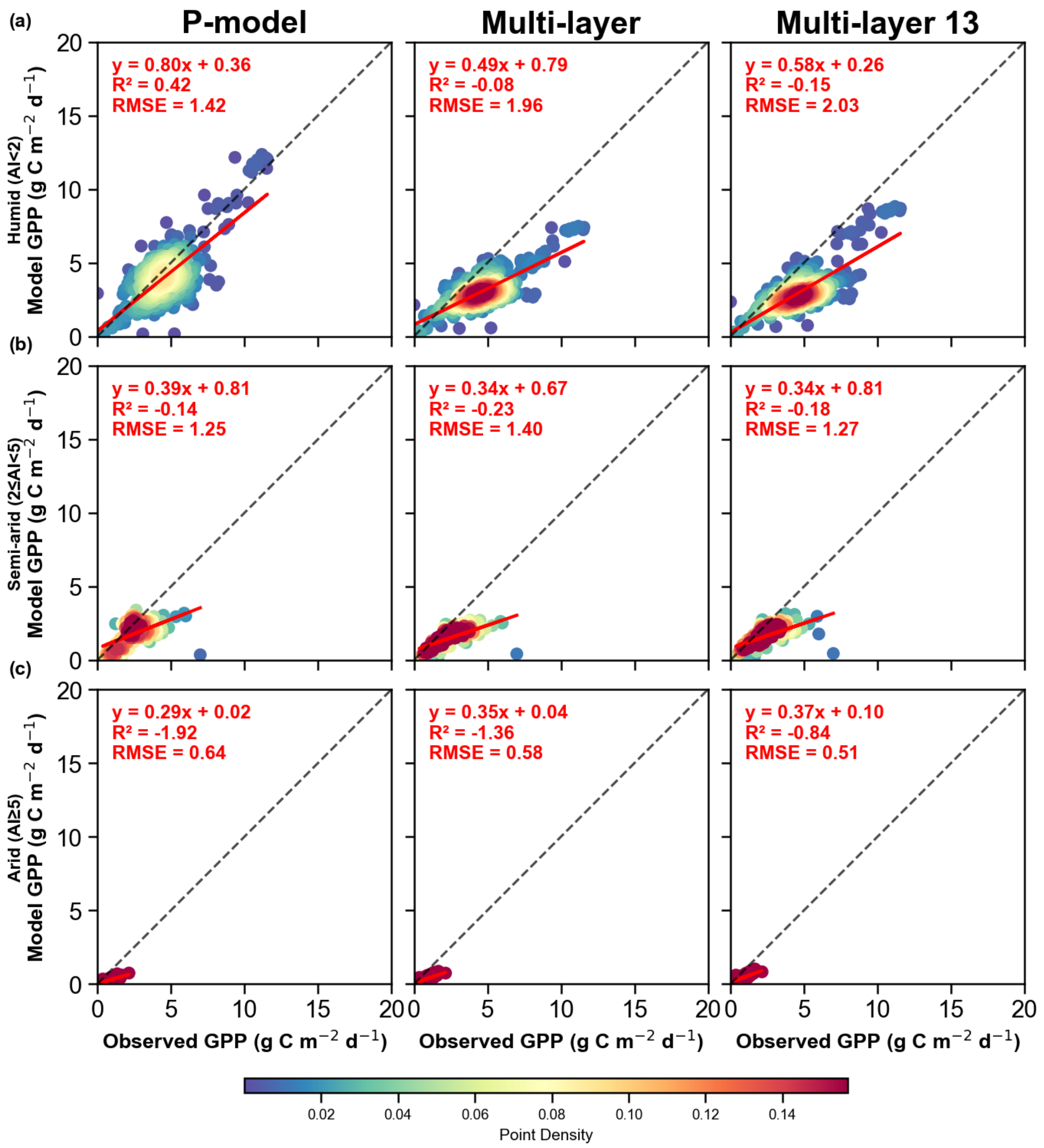

Figure S2. Simulated and observed seasonal cycle of gross primary production (GPP) at all tropical sites in PLUMBER2.

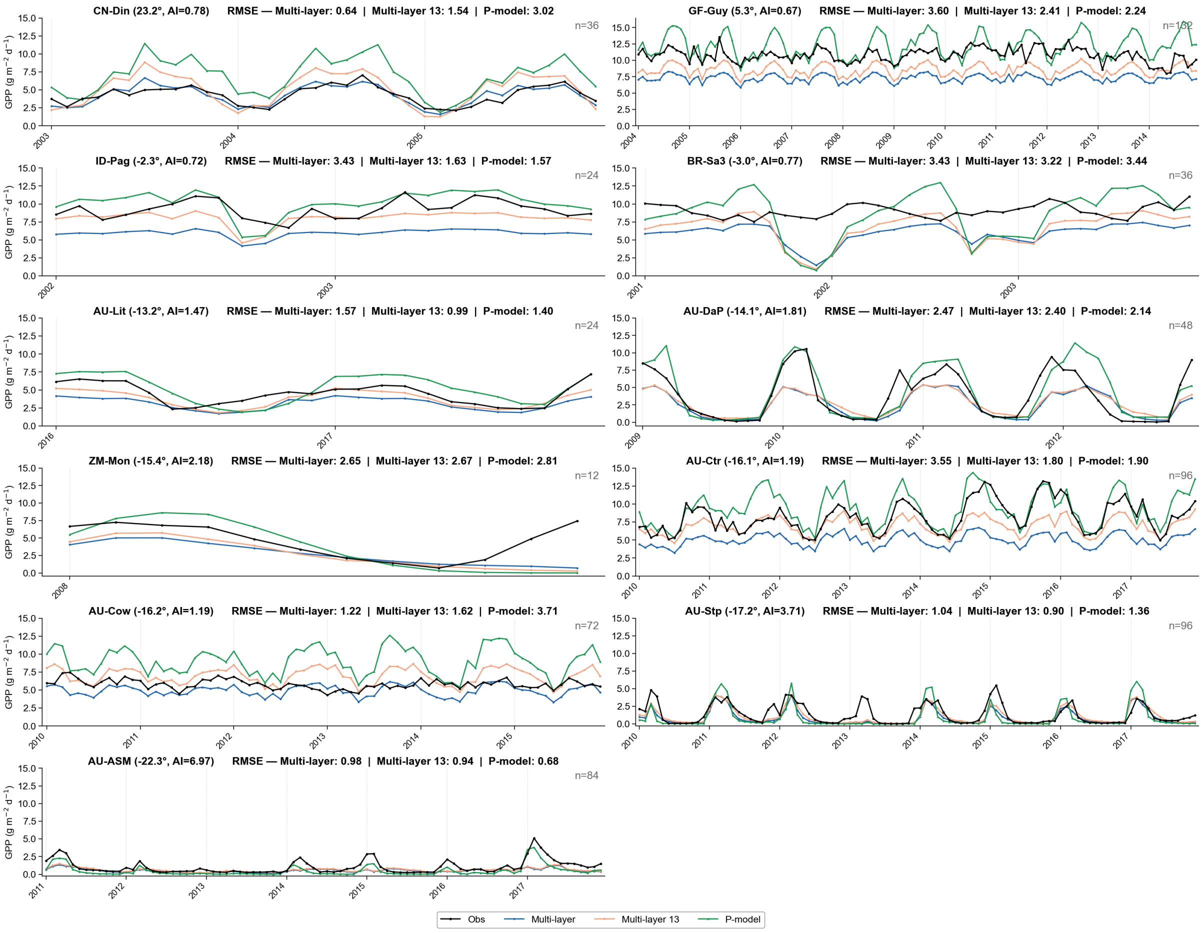

Figure S3. Simulated and observed seasonal cycle of leaf area index (LAI) at selected FLUXNET sites.

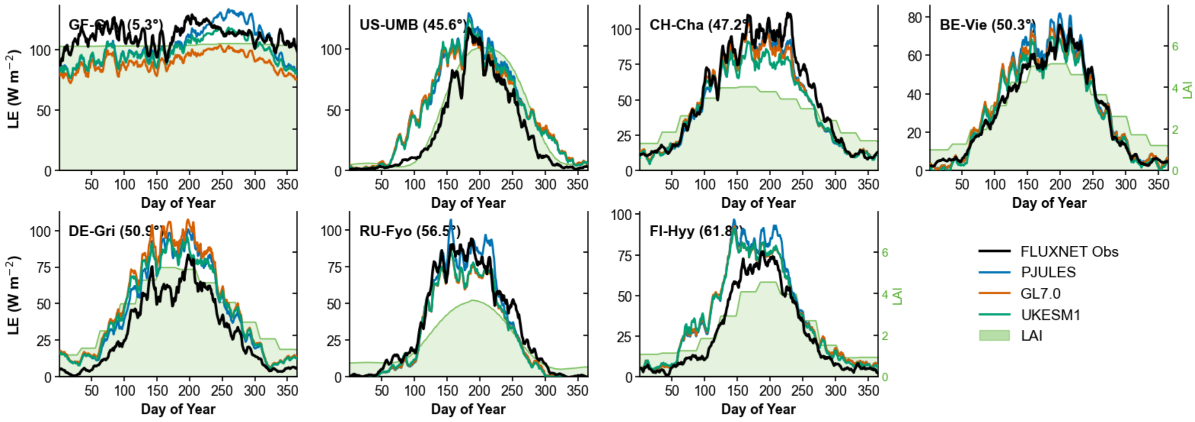

Table S1. Characteristics of the PLUMBER2 sites used in the analyses. Site code, observation period, geographic coordinates (latitude and longitude), elevation, data source, default leaf area index (LAI) source, and climatology aridity index (AI).

Site Code	Time Period	Latitude	Longitude	Elevation (m)	Data Source	Default LAI	AI
AR-SLu	2010	-33.4648	-66.4598	500	FLUXNET2015	MODIS	2.97
AT-Neu	2002-2012	47.11667	11.3175	970	FLUXNET2015	Copernicus	0.71
AU-ASM	2011-2017	-22.283	133.249	606	OzFlux	Copernicus	6.97
AU-Cow	2010-2015	-16.2382	145.4272	86	OzFlux	Copernicus	1.19
AU-Cpr	2011-2017	-34.0021	140.5891	76	OzFlux	MODIS	6.34
AU-Ctr	2010-2017	-16.1033	145.4469	66	OzFlux	MODIS	1.19
AU-Cum	2013-2018	-33.6133	150.7225	200	OzFlux	MODIS	1.56
AU-DaP	2011-2017	-14.0633	131.3181	116	OzFlux	Copernicus	1.81
AU-DaS	2010-2017	-14.1593	131.388	108	OzFlux	MODIS	1.81
AU-Dry	2011-2015	-15.2588	132.3706	191	OzFlux	Copernicus	2.32
AU-Emr	2012-2013	-23.8587	148.4746	177	OzFlux	Copernicus	3.09
AU-Gin	2012-2017	-31.375	115.65	51	OzFlux	MODIS	2.95
AU-GWW	2013-2017	-30.1913	120.6541	504	OzFlux	MODIS	5.77
AU-How	2003-2017	-12.4952	131.15	41	OzFlux	MODIS	1.45
AU-Lit	2016-2017	-13.179	130.7945	200	OzFlux	Copernicus	1.47
AU-Otw	2009-2010	-38.5323	142.8168	54	OzFlux	Copernicus	1.42
AU-Sam	2011-2017	-27.3881	152.8778	170	OzFlux	Copernicus	1.60
AU-Stp	2010-2017	-17.1507	133.3502	252	OzFlux	Copernicus	3.71
AU-TTE	2013-2017	-22.287	133.64	553	OzFlux	MODIS	7.20
AU-Tum	2002-2017	-35.6566	148.1517	1200	OzFlux	Copernicus	1.30
AU-Wrr	2016-2017	-43.095	146.6545	100	OzFlux	MODIS	0.81
AU-Ync	2011-2017	-34.9893	146.2907	125	OzFlux	Copernicus	3.97
BE-Bra	2004-2014	51.30917	4.52056	16	FLUXNET2015	MODIS	0.91
BE-Vie	1997-2014	50.30507	5.99805	493	FLUXNET2015	Copernicus	0.70
BR-Sa3	2001-2003	-3.01803	-54.9714	100	FLUXNET2015	MODIS	0.77
BW-Ma1	2000	-19.9165	23.56033	929	LaThuile	MODIS	4.44

CA-Qfo	2004-2010	49.6925	-74.3421	382	FLUXNET2015	Copernicus	0.68
CH-Cha	2006-2014	47.21022	8.41044	393	FLUXNET2015	Copernicus	0.73
CH-Dav	1997-2014	46.81533	9.85592	1639	FLUXNET2015	Copernicus	0.62
CH-Fru	2007-2014	47.11583	8.53778	982	FLUXNET2015	MODIS	0.69
CH-Oe1	2002-2008	47.28583	7.73194	450	FLUXNET2015	MODIS	0.81
CN-Cha	2003-2005	42.4025	128.0958	754	FLUXNET2015	MODIS	1.29
CN-Cng	2008-2009	44.5934	123.5092	138	FLUXNET2015	MODIS	2.40
CN-Dan	2004-2005	30.4978	91.0664	4751	FLUXNET2015	MODIS	3.42
CN-Din	2003-2005	23.1733	112.5361	261	FLUXNET2015	Copernicus	0.78
CN-Du2	2007-2008	42.0467	116.2836	1331	FLUXNET2015	MODIS	2.69
CN-HaM	2002-2003	37.37	101.18	3975	FLUXNET2015	MODIS	2.22
CN-Qia	2003-2005	26.7414	115.0581	64	FLUXNET2015	MODIS	0.81
CZ-wet	2007-2014	49.02465	14.77035	426	FLUXNET2015	MODIS	1.17
DE-Bay	1997-1999	50.14194	11.86694	781	LaThuile	Copernicus	1.04
DE-Gri	2004-2014	50.94947	13.51253	385	FLUXNET2015	Copernicus	1.19
DE-Hai	2000-2012	51.07917	10.453	430	FLUXNET2015	Copernicus	0.95
DE-Meh	2004-2006	51.27531	10.65547	291	LaThuile	MODIS	1.19
DE-Obe	2008-2014	50.78666	13.72129	734	FLUXNET2015	Copernicus	1.19
DE-Tha	1998-2014	50.96361	13.56694	380	FLUXNET2015	Copernicus	1.19
DE-Wet	2002-2006	50.4535	11.45753	703	LaThuile	MODIS	1.09
DK-Lva	2005-2006	55.6833	12.0833	-2493	LaThuile	Copernicus	1.10
DK-Sor	1997-2014	55.48587	11.64464	40	FLUXNET2015	Copernicus	1.15
DK-ZaH	2000-2013	74.47328	-20.5503	38	FLUXNET2015	MODIS	0.62
ES-ES1	1999-2006	39.34597	-0.31881	1	LaThuile	MODIS	3.19
ES-LgS	2007	37.09793	-2.96583	2267	FLUXNET2015	MODIS	2.67
ES-LMa	2004-2006	39.9415	-5.77336	278	LaThuile	MODIS	3.76
ES-VDA	2004	42.15218	1.4485	1787	LaThuile	MODIS	1.21
FI-Hyy	1996-2014	61.8475	24.295	181	FLUXNET2015	Copernicus	0.87
FI-Kaa	2000-2002	69.14069	27.29503	159	LaThuile	MODIS	0.77
FI-Lom	2007-2009	67.9972	24.20918	274	FLUXNET2015	MODIS	0.76

FI-Sod	2008-2014	67.36186	26.63783	180	FLUXNET2015	Copernicus	0.71
FR-Fon	2005-2013	48.4764	2.78014	103	FLUXNET2015	MODIS	1.40
FR-Hes	1997-2006	48.67416	7.06556	293	LaThuile	Copernicus	1.13
FR-LBr	2003-2008	44.71711	-0.7693	61	FLUXNET2015	MODIS	1.10
FR-Lq1	2004-2006	45.64306	2.73583	1066	LaThuile	MODIS	0.99
FR-Lq2	2004-2006	45.63919	2.73703	1081	LaThuile	MODIS	0.99
FR-Pue	2000-2014	43.74139	3.59583	270	FLUXNET2015	MODIS	1.56
GF-Guy	2004-2014	5.278772	-52.9249	48	FLUXNET2015	Copernicus	0.67
HU-Bug	2003-2006	46.6911	19.6013	106	LaThuile	MODIS	1.76
ID-Pag	2002-2003	-2.345	114.0364	52	LaThuile	Copernicus	0.72
IE-Dri	2003-2005	51.98669	-8.75181	186	LaThuile	Copernicus	0.50
IT-Amp	2003-2006	41.9041	13.60516	991	LaThuile	MODIS	1.29
IT-CA1	2012-2013	42.38041	12.02656	200	FLUXNET2015	MODIS	1.54
IT-CA3	2012-2013	42.38	12.0222	197	FLUXNET2015	MODIS	1.54
IT-Col	2007-2014	41.84936	13.58814	1560	FLUXNET2015	MODIS	1.29
IT-Cpz	2001-2008	41.70525	12.37611	68	FLUXNET2015	MODIS	1.73
IT-Isp	2013-2014	45.81264	8.63358	210	FLUXNET2015	MODIS	0.80
IT-Lav	2005-2014	45.9562	11.28132	1353	FLUXNET2015	MODIS	1.09
IT-LMa	2003-2004	45.15258	7.58259	350	LaThuile	MODIS	1.21
IT-Mal	2003	46.11402	11.70334	1610	LaThuile	MODIS	0.88
IT-MBo	2003-2012	46.01468	11.04583	1550	FLUXNET2015	MODIS	1.13
IT-Noe	2004-2014	40.60618	8.15117	25	FLUXNET2015	MODIS	2.26
IT-Non	2002	44.69019	11.09109	14	LaThuile	MODIS	1.38
IT-PT1	2003-2004	45.20087	9.06104	60	FLUXNET2015	Copernicus	1.09
IT-Ren	2010-2013	46.58686	11.43369	1730	FLUXNET2015	MODIS	0.84
IT-Ro1	2002-2006	42.40812	11.93001	235	FLUXNET2015	MODIS	1.92
IT-Ro2	2002-2008	42.39026	11.92093	160	FLUXNET2015	MODIS	1.92
IT-SR2	2013-2014	43.73203	10.29095	4	FLUXNET2015	MODIS	1.35
IT-SRo	2003-2012	43.72786	10.28444	6	FLUXNET2015	MODIS	1.35
JP-SMF	2003-2006	35.2617	137.0788	199	FLUXNET2015	MODIS	0.65

NL-Ca1	2003-2006	51.971	4.927	1	LaThuile	MODIS	0.86
NL-Hor	2008-2011	52.24035	5.0713	2.2	FLUXNET2015	MODIS	0.84
NL-Loo	1997-2013	52.16658	5.74356	25	FLUXNET2015	Copernicus	0.85
PL-wet	2004-2005	52.7622	16.3094	55	LaThuile	MODIS	1.35
PT-Esp	2002-2004	38.6394	-8.6018	90	LaThuile	MODIS	2.09
PT-Mi1	2005	38.54064	-8.00006	230	LaThuile	MODIS	2.16
PT-Mi2	2005-2006	38.4765	-8.02455	193	LaThuile	MODIS	2.51
RU-Fyo	2003-2014	56.46153	32.92208	265	FLUXNET2015	MODIS	0.97
SD-Dem	2005-2009	13.2829	30.4783	500	FLUXNET2015	MODIS	6.42
SE-Deg	2002-2005	64.18197	19.55669	242	LaThuile	Copernicus	0.73
UK-Gri	2000-2001	56.60722	-3.79806	343	LaThuile	MODIS	0.39
UK-Ham	2004	51.15353	-0.8583	76	LaThuile	MODIS	0.88
US-AR1	2010-2012	36.4267	-99.42	611	FLUXNET2015	Copernicus	2.50
US-AR2	2010-2011	36.6358	-99.5975	646	FLUXNET2015	Copernicus	2.61
US-Aud	2003-2005	31.5907	-110.509	1466	LaThuile	MODIS	5.08
US-Bar	2005	44.06464	-71.2881	270	LaThuile	MODIS	0.61
US-Bkg	2005-2006	44.34529	-96.8362	495	LaThuile	MODIS	1.60
US-Blo	2000-2006	38.8953	-120.633	1315	FLUXNET2015	Copernicus	1.63
US-Cop	2002-2003	38.09	-109.39	1520	FLUXNET2015	Copernicus	4.03
US-GLE	2009-2014	41.3665	-106.24	3197	FLUXNET2015	Copernicus	2.90
US-Goo	2004-2006	34.2547	-89.8735	87	LaThuile	MODIS	0.94
US-Ha1	1992-2012	42.5378	-72.1715	340	FLUXNET2015	MODIS	0.80
US-Ho1	1996-2004	45.2041	-68.7402	72	LaThuile	MODIS	0.70
US-KS2	2003-2006	28.60858	-80.6715	3	FLUXNET2015	MODIS	1.20
US-Los	2000-2008	46.0827	-89.9792	480	FLUXNET2015	MODIS	0.98
US-Me2	2002-2014	44.4523	-121.557	1253	FLUXNET2015	Copernicus	0.87
US-Me4	1996-2000	44.4992	-121.622	922	LaThuile	MODIS	0.87
US-Me6	2011-2014	44.3233	-121.608	998	FLUXNET2015	MODIS	0.87
US-MMS	1999-2014	39.3232	-86.4131	275	FLUXNET2015	MODIS	0.93
US-MOz	2005-2006	38.74411	-92.2	212	LaThuile	MODIS	1.14

US-NR1	1999-2014	40.0329	-105.546	3050	FLUXNET2015	MODIS	2.44
US-PFa	1995-2014	45.9459	-90.2723	470	FLUXNET2015	MODIS	1.02
US-Prr	2011-2013	65.1237	-147.488	210	FLUXNET2015	MODIS	1.64
US-SP2	2000-2004	29.7648	-82.2448	46	LaThuile	Copernicus	1.18
US-SP3	1999-2004	29.75477	-82.1633	36	LaThuile	Copernicus	1.18
US-SRG	2009-2014	31.7894	-110.828	1291	FLUXNET2015	MODIS	5.08
US-SRM	2004-2014	31.8214	-110.866	1120	FLUXNET2015	MODIS	5.08
US-Syv	2002-2008	46.242	-89.3477	540	FLUXNET2015	MODIS	1.00
US-Ton	2001-2014	38.4316	-120.966	177	FLUXNET2015	MODIS	2.27
US-UMB	2000-2014	45.5598	-84.7138	234	FLUXNET2015	MODIS	0.98
US-Var	2001-2014	38.4133	-120.951	129	FLUXNET2015	MODIS	2.27
US-WCr	1999-2006	45.8059	-90.0799	520	FLUXNET2015	Copernicus	1.02
US-Whs	2008-2014	31.7438	-110.052	1370	FLUXNET2015	MODIS	5.88
US-Wkg	2005-2014	31.7365	-109.942	1531	FLUXNET2015	MODIS	6.29
ZA-Kru	2000-2002	-25.0197	31.4969	359	FLUXNET2015	MODIS	2.73
ZM-Mon	2008	-15.4378	23.25278	1053	FLUXNET2015	MODIS	2.18

Table S2. Comparison of the performance of PJULES and the JULES-UKESM1 multi-layer model across different PFTs.

PFT	Observations mean	PJULES Mean	PJULES RMSE	UKESM1 mean	UKESM1 RMSE
Broadleaf Deciduous	4.299	3.67	1.672	2.646	2.016
Broadleaf Evergreen Temperate	5.059	4.956	1.213	2.904	2.517
Broadleaf Evergreen Tropical	7.887	8.852	1.502	7.047	1.597
C3 Crop	3.546	2.674	1.495	2.345	1.496
C3 Grass	2.921	2.026	1.355	2	1.364
Needleleaf Evergreen	4.031	3.498	1.285	2.162	2.155
Shrub Deciduous	4.248	4.138	0.965	3.454	0.794

Table S3. Summary of seasonal model performance and statistical metrics for Gross Primary Productivity (GPP) in the Northern Hemisphere.

Season	Observed Mean GPP	Model	Mean GPP	R^2	RMSE
MAM	3.95	PJULES	5.09	0.39	2.65
		GL7.0	3	0.5	2.42
		UKESM1	2.83	0.47	2.47
JJA	7.2	PJULES	7.65	0.3	3.63
		GL7.0	4.64	0.09	4.2
		UKESM1	4.5	0.06	4.23
SON	3.21	PJULES	3.34	0.53	1.92
		GL7.0	2.09	0.5	1.98
		UKESM1	2.05	0.49	2
DJF	1.72	PJULES	1.62	0.7	1.39
		GL7.0	0.96	0.67	1.43
		UKESM1	0.95	0.67	1.48

Table S4. Summary of seasonal model performance and statistical metrics for gross primary production (GPP) simulations in the Southern Hemisphere.

Season	Observed mean GPP	Model	Mean GPP	R^2	RMSE
MAM	4.95	PJULES	5.17	0.47	1.96
		GL7.0	2.97	0.21	2.52
		UKESM1	3.44	0.16	2.47
JJA	3.33	PJULES	3.69	0.62	1.45
		GL7.0	2.22	0.56	1.67
		UKESM1	2.43	0.39	1.86
SON	4.97	PJULES	5.60	0.31	2.82
		GL7.0	3.14	0.46	2.68
		UKESM1	3.32	0.36	2.73
DJF	6.36	PJULES	6.64	0.05	3.32
		GL7.0	3.74	0.20	3.22
		UKESM1	4.33	0.18	3.10

Table S5. Summary of seasonal model performance and statistical metrics for latent heat (LE) in the Northern Hemisphere.

Season	**Observed mean LE**	**Model**	**Mean LE**	**R^2**	**RMSE**
MAM	38.26	PJULES	48.16	0.31	20.53
		GL7.0	48.5	0.28	21.16
		UKESM1	46.93	0.36	19.81
JJA	68.32	PJULES	76.48	0.14	27.47
		GL7.0	69.53	0.27	25.57
		UKESM1	68.71	0.28	25.12
SON	27.93	PJULES	32.65	0.55	15.09
		GL7.0	32.13	0.55	15.19
		UKESM1	31.66	0.6	14.36
DJF	13.04	PJULES	14.88	0.54	10.9
		GL7.0	15.13	0.51	11.17
		UKESM1	14.29	0.58	10.5

Table S6. Summary of seasonal model performance and statistical metrics for latent heat (LE) in the Southern Hemisphere.

Season	Observed mean LE	Model	Mean_LE	R^2	RMSE
MAM	68.03	PJULES	64.82	0.55	24.06
		GL7.0	52.94	0.42	26.42
		UKESM1	60.67	0.57	23.54
JJA	43.35	PJULES	37.69	0.5	20.42
		GL7.0	34.81	0.44	22.15
		UKESM1	37.6	0.47	21.15
SON	62.48	PJULES	61.91	0.6	21.74
		GL7.0	53.96	0.66	19.67
		UKESM1	59.28	0.67	19.9
DJF	91.3	PJULES	91.18	0.42	25.42
		GL7.0	77.04	0.34	26.58
		UKESM1	86.33	0.54	22.56

Note S1. Photosynthesis in JULES

The gross photosynthesis rate (W) for C_3 plants is based on the biochemical formulations of Collatz et al. (1991). The gross photosynthetic rate is determined by the smoothed minimum of three potentially limiting rates: the Rubisco-limited rate (W_c), the light-limited rate (W_l), and the rate of transport of photosynthetic products (W_e).

The rate of photosynthesis limited by the carboxylation capacity of Rubisco is calculated as:

$$W_c = V_{cmax}\left(\frac{c_i - \Gamma}{c_i + K_c(1 + O_a/K_o)}\right) \qquad \text{Eqn.S1}$$

V_{cmax} (mol CO_2 m^{-2} s^{-1}) represents the maximum rate of carboxylation of Rubisco, and c_i (Pa) is the leaf internal CO_2 partial pressure. The variable Γ (Pa) denotes the CO_2 compensation point in the absence of mitochondrial respiration, while O_a (Pa) stands for the partial pressure of atmospheric oxygen. Additionally, K_c and K_o (Pa) are the Michaelis-Menten parameters for CO_2 and O_2, respectively.

The rate of photosynthesis limited by the amount of absorbed photosynthetically active radiation (PAR) is:

$$W_l = \alpha(1 - \omega)I_{par}\left(\frac{c_i - \Gamma}{c_i + 2\Gamma}\right) \qquad \text{Eqn.S2}$$

Here, α (mol CO_2 mol^{-1} PAR) defines the quantum efficiency of photosynthesis, and ω represents the leaf scattering coefficient for PAR. Ipar (mol m^{-2} s^{-1}) is the incident photosynthetically active radiation.

The rate limited by the transport of photosynthetic products (triose phosphate utilization) is calculated as:

$$W_e = 0.5V_{cmax} \qquad \text{Eqn.S3}$$

To account for the smooth transition between these three limiting states, W) is calculated by solving two nested quadratic equations. First, W_p of the Rubisco- and light-limited rates is determined by finding the smaller root of:

$$\beta_1 W_p^2 - W_p(W_c + W_l) + W_c W_l = 0 \qquad \text{Eqn.S4}$$

where $\beta_1 = 0.83$ serves as a co-limitation coefficient.

The gross photosynthesis rate (W) is calculated as the smoothed minimum of W_p and the W_e by finding the smaller root of:

$$\beta_2 W^2 - W(W_p + W_e) + W_p W_e = 0 \qquad \text{Eqn.S5}$$

where β_2 = 0.93 is the second co-limitation coefficient.

The biochemical parameters Vcmax, Kc, Ko, and Γ are strongly dependent on the canopy (leaf) temperature (Tc, in °C).

The CO2 photorespiration compensation point (Γ) is defined as:

$$\Gamma = \frac{O_a}{2\tau} \qquad \text{Eqn.S6}$$

where τ represents the Rubisco specificity for CO_2 relative to O_2, calculated as:

$$\tau = 2600 \cdot Q_{10_{rs}}^{0.1(T_c - 25)} \qquad \text{Eqn.S7}$$

with $Q10_{rs}$ = 0.57.

Finally, the Michaelis-Menten parameters are calculated as:

$$K_c = 30 \cdot Q_{10_{Kc}}^{0.1(T_c - 25)} \qquad \text{Eqn.S8}$$

$$K_o = 3 \times 10^4 \cdot Q_{10_{Ko}}^{0.1(T_c - 25)} \qquad \text{Eqn.S9}$$

where the temperature dependence constants $Q_{10_{Kc}}$ and $Q_{10_{Ko}}$ are assigned values of 2.1 and 1.2, respectively.

The dimensionless moisture stress factor (β) is related to the mean soil moisture concentration in the root zone (θ), as well as the critical (θ_{crit}) and wilting point (θ_w) concentrations. It is calculated as follows:

$$\beta = \begin{cases} 1 & (\text{for } \theta \geq \theta_{\text{crit}}) \\ \frac{\theta - \theta_w}{\theta_{crit} - \theta_w} & (\text{for } \theta_w < \theta < \theta_{\text{crit}}) \\ 0 & (\text{for } \theta \leq \theta_w) \end{cases} \qquad \text{Eqn.S10}$$

The critical threshold (θ_{crit}) in this model corresponds to a matric potential of -33 kPa (Cox et al., 1999).

The total fluxes at the canopy scale are derived by aggregating the corresponding leaf-level fluxes across all vertical layers, weighted by the leaf area of each respective layer.

Therefore, the gross photosynthetic rate for a given individual canopy layer (A_i) is calculated by multiplying the leaf-level assimilation rate ($A_{l,i}$) by the leaf area increment of that specific layer (dL_c):

$$A_i = A_{\mathrm{l,i}} dL_{\mathrm{c}} \quad \text{Eqn.S11}$$

The total canopy-level photosynthesis (A_{total}) is then obtained by summing the contributions from all n layers within the canopy:

$$A_{\mathrm{total}} = \sum_{i=1}^{n} A_{\mathrm{i}} \quad \text{Eqn.S12}$$

Since the model configuration accounts for canopy light penetration (sunflecks) and explicitly distinguishes between sunlit and shaded foliage, the layer-specific photosynthesis (A_i) is partitioned accordingly. It is computed as the area-weighted average of assimilation by sunlit ($A_{sun,i}$) and shaded ($A_{sh,i}$) leaves, driven by the sunlit fraction ($f_{sun,i}$) of that layer:

$$A_{\mathrm{i}} = f_{\mathrm{sun,i}} A_{\mathrm{sun,i}} + (1 - f_{\mathrm{sun,i}}) A_{\mathrm{sh,i}} \quad \text{Eqn.S13}$$

Note S2. Sub-daily P-model description

The sub-daily P model (Mengoli et al., 2022) builds on the P model framework (Prentice et al., 2014; Wang et al., 2017; Stocker et al., 2020) by explicitly separating the instantaneous and acclimated responses of photosynthetic responses to environmental variation. Acclimated variables are acclimated V_{cmax25} ($V_{\mathrm{cmax25,acclim}}$) and J_{max25} ($J_{\mathrm{max25,acclim}}$) the optimal stomatal parameter ξ.

To simulate the instantaneous response, gross photosynthesis is calculated as the minimum of the Rubisco-limited rate and the light-limited rate, following the Farquhar–von Caemmerer–Berry model of C_3 photosynthesis (FvCB: Farquhar et al., 1980). The Rubisco-limited rate, representing the rate of CO_2 fixation determined by the amount and catalytic activity of Rubisco, is given by:

$$A_c = V_{cmax} \times \frac{(c_i - \Gamma^*)}{(c_i + K)}$$ Eqn.S14

And the light-limited rate is given by:

$$A_J = \frac{J}{4} \times \frac{(c_i - \Gamma^*)}{(c_i + 2\Gamma^*)}$$ Eqn. S15

where V_{cmax} represents the maximum rate of Rubisco carboxylation, J represents the electron-transport rate and c_i is the leaf-internal CO_2 partial pressure. Here, instantaneous c_i is mainly determined by two variables, the current leaf-to-air vapour pressure deficit (VPD) and the acclimated optimal stomatal parameter ξ (Eqn. S28). ξ is kept constant over the diurnal cycle, since this is a trait that adjusts on acclimation timescales rather than responding instantaneously to short-term fluctuations in environmental drivers. Γ^* is the photorespiratory CO_2 compensation point, and K is the effective Michaelis–Menten coefficient of Rubisco. The electron transport rate J is calculated as:

$$J = \frac{4\varphi_0 I_{abs}}{\sqrt{1+(\frac{4\varphi_0 I_{abs}}{J_{max}})^2}}$$ Eqn. S16

$\varphi_0(T)$ is given by:

$$\phi_0(T) = \frac{1}{8} \times (0.352 + 0.022 \cdot T - 0.00034 \cdot T^2)$$ Eqn. S17

where φ_0 is the intrinsic quantum efficiency and T is temperature (K).

Temperature sensitivities for Γ* and K are taken from Farquhar et al. (1980) and Bernacchi et al. (2001). $\Gamma^*(T)$ is calculated from the CO_2 compensation point at 25°C (Γ^*_{25}) as:

$$\Gamma^*(T) = \Gamma^*_{25} \cdot \exp\frac{(T - 25) \cdot E_{a,\Gamma^*}}{R \cdot 298(T+273.15)} \cdot \frac{Patm}{Pa(O)}$$ Eqn. S18

where Γ^*_{25}= 4.332 Pa, $E_{a,\Gamma}{}^*$ = 37830 J mol^{-1} is the activation energy for Γ^*, R = 8.314 J mol^{-1} K^{-1} is the universal gas constant (Farquhar et al., 1980). P_{atm} is surface air pressure and P(O) is the partial pressure of oxygen.

K is calculated from the Michaelis-Menten constants for carboxylation (K_c) and oxygenation (K_o):

$$K = K_c(1 + \frac{P(O)}{K_o})$$ Eqn. S19

The temperature dependencies of K_c and K_o are given by:

$$K_c(T) = K_{c,25} \cdot \exp \frac{(T - 25) \cdot E_{a,kc}}{R \cdot 298(T + 273.15)}$$ Eqn. S20

and

$$K_o(T) = K_{o,25} \cdot \exp \frac{(T - 25) \cdot E_{a,ko}}{R \cdot 298(T + 273.15)}$$ Eqn. S21

where $K_{c,25}$ is the Michaelis–Menten constant for Rubisco carboxylation at 25 °C and $K_{o,25}$ at 25 °C is the Michaelis–Menten constant for Rubisco oxygenation at 25 °C. $K_{c,25}$ and $K_{o,25}$ are set to 39.97 Pa and 27 480 Pa, respectively. $E_{a,kc}$ and $E_{a,ko}$ are the activation energies for K_c and K_o, set to 79 430 and 36 380 J mol^{-1}, respectively.

Net photosynthesis rate is calculated as:

$$A_{net} = A - R_d$$ Eqn. S22

where leaf dark respiration (R_d) is estimated as:

$$R_d = 0.015 \times V_{cmax}$$ Eqn. S23

The instantaneous values of V_{cmax} and J_{max} are adjusted for the current leaf temperature (T_{ins}) using standard Arrhenius equations:

$$V_{cmax}(T_{ins}) = V_{cmax25,acclim} \times \exp(\frac{E_{a,c}}{R} \times \frac{T_{ins} - 298.15}{T_{ins} \times 298.15})$$ Eqn. S24

$$J_{max}(T_{ins}) = J_{max25,acclim} \times \exp(\frac{E_{a,J}}{R} \times \frac{T_{ins} - 298.15}{T_{ins} \times 298.15})$$ Eqn. S25

where $E_{a,c}$ = 65330 J mol^{-1} is the activation energy for V_{cmax} (Bernacchi et al., 2001), and $E_{a,J}$ = 43900 J mol^{-1} is the activation energy for J_{max} (Bernacchi et al., 2003).

The $V_{cmax25,acclim}$ and $J_{max25,acclim}$ values were calculated by applying the inverse form of the Arrhenius equation to $V_{cmax,opt}$ and $J_{max,opt}$ at the acclimated temperature (T_{accl}):

$$V_{cmax25,acclim}(T_{accl}) = V_{cmax,opt} \times \exp(\frac{E_{a,c}}{R} \times \frac{298.15 - T_{accl}}{T_{accl} \times 298.15}) \quad \text{Eqn. S26}$$

$$J_{max25,acclim}(T_{accl}) = J_{max,opt} \times \exp(\frac{E_{a,J}}{R} \times \frac{298.15 - T_{accl}}{T_{accl} \times 298.15}) \quad \text{Eqn. S27}$$

where V_{cmax} and J_{max} represent the V_{cmax} and J_{max} at the average midday (11:30–12:30 local solar time, corresponding to the period of peak irradiance) environmental conditions during the previous 15 days as well as the T_{accl}.

$V_{cmax,opt}$ and $J_{max,opt}$ are determined using two optimality principles. According to the coordination hypothesis, plants adjust their photosynthetic capacities so that A_J is approximately equal to A_C under typical/average daytime conditions, ensuring efficient use of available light. The least-cost hypothesis predicts that c_i adjusts in response to ambient CO_2 partial pressure (c_a), vapor pressure deficit (VPD), temperature, and atmospheric pressure, thereby determining the value of the stomatal parameter (ξ) that balances carbon assimilation and water loss (Eqn. S31). A higher ξ reduces the sensitivity of c_i to changes in VPD. This balance minimises the combined costs of carboxylation and water transport required to sustain a given assimilation rate:

$$\xi = \sqrt{\frac{\beta(K + \Gamma^*)}{1.6\eta^*}} \quad \text{Eqn. S28}$$

β is the unitless cost ratio at 25℃ for maintaining carboxylation and water transport, set to 146 following Wang et al. (2017). $\eta*$ is the unitless ratio of the viscosity of water at a given temperature relative to its viscosity at 25 °C (Huber et al., 2009).

From the equation above, we can derive $V_{cmax,opt}$, $J_{max,opt}$ and $c_{i,opt}$:

$$V_{cmax,opt} = \frac{\varphi_0 I_{abs}[(c_{i,opt} + K)}{(c_{i,opt} + 2\Gamma^*)} \sqrt{\left\{1 - [c^* \frac{(c_{i,opt} + 2\Gamma^*)}{(c_{i,opt} - \Gamma^*)}]^{\frac{2}{3}}\right\}}$$ Eqn. S29

$$J_{max,opt} = \frac{4\varphi_0 I_{abs}}{\sqrt{\frac{1}{\left\{1 - [c^* \frac{(c_{i,opt} + 2\Gamma^*)}{(c_{i,opt} - \Gamma^*)}]^{\frac{2}{3}}\right\}} - 1}}$$ Eqn. S30

where $c_{i,opt}$ is the leaf-internal CO_2 partial pressure corresponding to the optimal environmental conditions at which $V_{cmax,opt}$, $J_{max,opt}$ are determined.

$$c_{i,opt} = \frac{\xi C_a + \Gamma^* \sqrt{VPD}}{\xi + \sqrt{VPD}}$$ Eqn. S31

where c^* is a cost factor for electron transport capacity and has been estimated as 0.41 ± 0.112 from observed J_{max}:V_{max} ratios (Wang et al., 2017).